Local Ordering in Liquids: Solvent Effects on the Hyperfine Couplings of the Cyclohexadienyl Radical

Danilo Vujošević,[†] Herbert Dilger,[†] Iain McKenzie,[†,‡] Aleksandra Martyniak,[†] Robert Scheuermann,[§] and Emil Roduner*[,†]

Institut für Physikalische Chemie, Universität Stuttgart, Pfaffenwaldring 55, D-70569 Stuttgart, Germany, and Laboratory for Muon Spin Spectroscopy, Paul Scherrer Institute, CH-5232 Villigen, Switzerland

Received: August 24, 2006; In Final Form: October 5, 2006

Ordering of solvent molecules in the vicinity of a dipolar free radical affects its hyperfine coupling constants (hfcs). Specifically, it is demonstrated how the variation of the experimental methylene proton and muon hfcs of the muoniated cyclohexadienyl radical in several solvents and solvent mixtures of varying polarity can be accounted for by a dipole−dipole reaction field model that is based on the model of Reddoch and Konishi (*J. Chem. Phys.* **1979**, *70*, 2121) which was developed to explain the solvent dependence of the ^{14}N hfc in the di-*tert*-butyl-nitroxide radical. Ab initio calculations were carried out with the cyclohexadienyl radical in an electric field to model the electric field arising from the electric dipole moments of the surrounding solvent molecules. An extension of the model that includes the dipole−quadrupole interaction can account for the larger hfc in benzene compared with that in octadecane, and it is predicted that the hfc will be proportional to the concentration of quadrupole moments to the 4/3 power. The influence of hydrogen bonding between the radicals' π electrons and the OH groups of the solvent on the hfcs is also discussed. Comparison with gas-phase data permits a separation of vibrational effects and reveals that approximately 28% of the temperature dependence in water is due to increasing solvent disorder.

Introduction

An appropriate solvent can significantly increase the rate of formation and the product yield in organic synthesis.[1−4] The changes in reaction rates are the results of solvent stabilization of reactants or transition states, accompanied by changes in their geometric and electronic structures. The hyperfine coupling constants (hfcs) are a sensitive means of examining the electronic structure of a radical and monitoring how this is altered through solvent interactions. There have been many studies of solvent effects on stable free radicals such as di-*tert*-butyl-nitroxide (DTBN), and the results have been typically interpreted in terms of a reaction field model. Solute−solvent interactions are most commonly described by various continuum models,[5] basically inspired by those of Onsager[6] and Kirkwood.[7] Common for all of them is that they use the dielectric constant as the property that determines solvent−solute interaction. For example, when applying the continuum model approach to radicals, Al-Bala'a and Bates found that the hfc correlates linearly with $(\epsilon - 1)/(\epsilon + 1)$, where ϵ is the solvent dielectric constant.[8] Recently, the conventional theoretical dielectric continuum description of dipolar solvents has been extended to include effects arising from the molecular quadrupole moment of non-dipolar solvents,[9] but the treatment has not been tested for its suitability to describe solvent effects on hyperfine couplings. The main problem with most continuum solvation models is that the interaction energy saturates too quickly with increasing ϵ and that they do not take explicit solute−solvent interactions into account. Further criticisms can be found elsewhere.[10] Improvements in using the continuum model have been made by calculating a "local" dielectric constant,[11] but in this sense, ϵ loses its meaning since it is defined as a bulk property. Once solvation is understood, the hfc may be used as a probe of the radical's environment.[12,13]

Reddoch and Konishi (henceforth abbreviated as RK) developed a dipole−dipole reaction field model to account for the solvent dependence of the ^{14}N hfc (A_N) in DTBN,[10] that has advantages in comparison to the continuum solvation models. The RK model serves as the basis of the present study. The authors used a modified Hückel molecular orbital treatment to demonstrate that the ^{14}N hfc is linearly dependent on the electrostatic potential difference (ΔU) between the oxygen and the nitrogen atoms

$$A_N = A_N^0 + C r_{NO} \Delta U \tag{1}$$

where C is a constant typical for the given radical and r_{NO} is the distance between the nitrogen and oxygen atoms. The bulky *tert*-butyl substituents of DTBN protect the NO group from all sides except one, and the reaction field is dominated by a single solvent molecule on the axis of the NO bond. RK calculated the additional electric field at the center of the NO group that is due to the dipole moment of the nearest solvent molecule and concluded that A_N depends linearly on the product of the magnitude and the concentration of solvent dipole moments, abbreviated as $[\mu_S]$,

$$A_N = A + B\mu_S \frac{\rho_S}{M_S} = A + B[\mu_S] \tag{2}$$

where A and B are empirical constants that depend on the type of radical, μ_S is the dipole moment of the solvent molecule,

[†] Universität Stuttgart.
[‡] Present address: ISIS, Rutherford Appleton Laboratory, Chilton, Didcot, U.K.
[§] Paul Scherrer Institute.

10.1021/jp065488q CCC: $37.00
Published on Web 01/04/2007

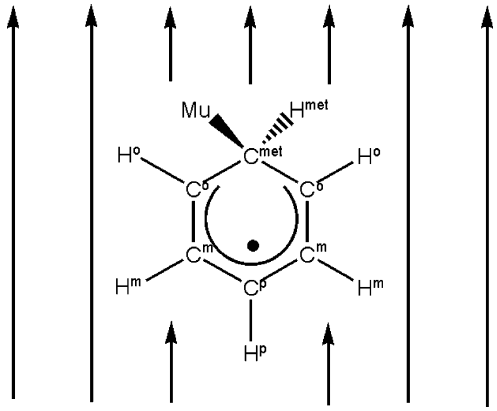

Figure 1. Cyclohexadienyl radical in an electric field with a direction shown by the arrows. One methylene proton, H^{met}, is replaced by the lightest hydrogen isotope muonium (Mu).

and ρ_S and M_S are the density and the molecular weight of the solvent, respectively. RK suggested that their model could be valid for other radicals but that the constants in the derived equations would be different for each particular radical.[10]

The partitioning of substituted cyclohexadienyl radicals at surfactant bilayer/water interfaces has recently been studied using muon spin resonance spectroscopy,[12−14] and the hfcs of these radicals were observed to depend strongly on the solvent.[15] The significant solvent effects in these substituted radicals have motivated us to investigate the simpler unsubstituted cyclohexadienyl radical. Experimental studies of the cyclohexadienyl radical (C_6H_7) are typically very challenging owing to its high reactivity and the difficulty in producing it.[16] It has been observed by electron paramagnetic resonance upon irradiation of 1,4-cyclohexadiene[17] and solid benzene, but the temperature range and solvents in which it could be studied are extremely limited.

It is advantageous to study the muoniated isotopologue of the cyclohexadienyl radical (C_6H_6Mu), as this radical can be produced in many different solvents and over a wide temperature range. Muoniated radicals contain a positive muon (μ^+) as a polarized spin label. The positive muon is an elementary particle with a spin of 1/2, a lifetime of 2.2 μs, a mass approximately one-ninth that of the proton, and a magnetic moment 3.18 times that of the proton which makes it a very sensitive magnetic probe. In beams of almost 100% spin polarization, monoenergetic muons are available at several accelerator facilities throughout the world. Muons can easily be implanted into solid, liquid, or gaseous samples, and a fraction of these muons can pick up an electron during the radiolysis process to form a one-electron hydrogen-like atom that is called muonium (Mu). The reduced mass and ionization potential of H and Mu are almost the same, which means that the chemical properties are also almost the same, so Mu can be considered an isotope of H, just like D or T. Mu reacts rapidly with benzene to give the C_6H_6Mu radical (shown in Figure 1). The muon and proton hfcs of C_6H_6Mu have been measured in the gas phase and in pure benzene over a wide temperature range,[18−21] but there is no information on the hfcs in other solvents. In this study, we measure the hfcs of the methylene muon (A_μ^{met}) and of the methylene proton (A_p^{met}; see Figure 1 where H^{met}, C^o, H^o, C^m, H^m, C^p, and H^p denote the methylene proton, and the ortho, meta, and para carbon and hydrogen atoms with respect to the methylene hydrogen) since it is the largest, making it the most suitable for studying the solvent effects that usually give small relative shifts of the hfc.[10,22] The hfcs of the in-plane protons in C_6H_6Mu were not measured since they, and consequently their solvent shifts, are much smaller. In some cases, it is necessary to distinguish between the muoniated and the non-muoniated isotopologues as the light mass of Mu can have a large effect on the structure and dynamics. Normally, however, C_6H_7 will be used synonymously with C_6H_6Mu, and no distinction is made between the two species in the models. The effect of Mu substitution on the cyclohexadienyl radical is well understood; the main effect is that the C−Mu bond is elongated by approximately 4.9% because of the increased zero-point energy while the methylene proton bond is almost unchanged.[19] This allows us to directly relate A_p^{met} of C_6H_6Mu to that of C_6H_7, and we will generally talk about C_6H_7 except when we specifically mention C_6H_6Mu.

There are several magnetic resonance techniques that are based on the parity violating decay of the positive muon. They are collectively known as μSR, which stands for muon spin rotation, resonance, and relaxation. The muon decay produces a positron (e^+) and two neutrinos, and the positron is emitted preferentially along the direction of the muon's spin. The detection of the decay positrons as a function of time provides a convenient means of monitoring the evolution of the muon's spin. In this study, the A_p^{met} has been measured by avoided level crossing muon spin resonance (ALC-μSR). One advantage of this technique is that it can be used in very dilute samples. In this experiment, muons are injected into the sample with their spin collinear to the magnetic field. It is run in a time-integral mode; that is, the number of positrons emitted in the forward and backward directions with respect to the incoming muon beam (N_F and N_B, respectively) is counted as a function of the applied magnetic field. The asymmetry is given by $(N_B - N_F)/(N_B + N_F)$. At specific values of the applied field, nearly degenerate pairs of spin states can mix through the hyperfine interaction, causing the muon polarization to oscillate between the two mixing states and resulting in a resonant-like change in the asymmetry as the magnetic field is swept. There are three types of ALC-μSR resonances, denoted Δ_0, Δ_1, and Δ_2, where the subscript refers to the change of the sum of the quantum numbers for the z-components of the muon and nuclear spins. In isotropic environments, only Δ_0 ALC-μSR resonances are observed, and their resonance field, B_r, depends on the muon (A_μ) and proton (A_p) hfcs as

$$B_r(\Delta_0) = \left|\frac{A_\mu - A_p}{2(\gamma_\mu - \gamma_e)} - \frac{A_\mu - A_p}{2\gamma_e}\right| \qquad (3)$$

Objectives. An objective of this study is to further develop the dipole−dipole reaction field model of RK[10] and to apply it to describe the solute−solvent interactions for the C_6H_7 radical. It is instructive to compare DTBN and C_6H_7 to see what the differences and similarities are between them.

One of the main points of the dipole−dipole reaction field theory is that the ^{14}N hfc in DTBN is directly proportional to the potential difference along the NO group electric dipole moment axis. For symmetry reasons, there are no other components which could play a role. The RK model assumes that the primary dipole moment of the radical induces some degree of preferential alignment in the orientation of the surrounding solvent dipoles, which then produces an electric field that alters the hfcs. In order to test to what extent this affects the hfcs of C_6H_7, ab initio calculations were performed with different applied electric fields along the C_6H_7 dipole moment axis, as shown in Figure 1.

It is expected that the electric field influences the electronic structure, which in turn alters the hfcs. In order to distinguish

TABLE 1: Numerically Extrapolated Δ_0 ALC Resonance Field Positions of Cyclohexadienyl Radical Methylene Proton at 308 K and at 348 K in Various Solvents and Mixtures

solvent[a]	$[\mu_S]$ (D mol dm^{-3})	B_r (G); A_p^{met} (MHz) ($T = 308$ K)	B_r (G); A_p^{met} (MHz) ($T = 348$ K)	$\Delta B_r/\Delta T$ (G K^{-1})	$\Delta A_p^{met}/\Delta T$ (MHz K^{-1})
octadecane	0	20635; 126.00	20507; 125.22	−3.15	−0.0192
$^1/_2$EtOH/$^1/_2$octanol	21.0	20704; 126.42	20577; 125.64	−3.17(4)	−0.0193(2)
EtOH	30.6	20725; 126.55	20591; 125.73	−3.25(4)	−0.0199(3)
MeOH	44.0	20750; 126.70	20615; 125.88	−3.30(1)	−0.0202(7)
$^1/_3$H$_2$O/$^2/_3$MeOH	63.7	20815; 127.10	20686; 126.31	−3.16(7)	−0.0193(4)
$^2/_3$H$_2$O/$^1/_3$MeOH	83.4	20880; 127.49	20749; 126.69	−3.20(7)	−0.0195(4)
H$_2$O	103.1	20931; 127.81	20807; 127.05	−3.00(7)	−0.0183(4)
benzene	0	20716; 126.49	20569; 125.59	−3.60(7)	−0.0219(5)

[a] MeOH (methanol), EtOH (ethanol), and OctOH (octanol).

the contribution of the geometric differences in environments of different polarity, two series of ab initio calculations were performed. In one series, the structure of C_6H_7 was optimized in the applied electric field. In the second series, the optimized structures for the given values of the electric field were used but with the electric field turned off, and the A_p^{met} values obtained in the two series were compared.

One major shortcoming of the dipole−dipole reaction field model is that it is valid only for dipolar liquids and cannot account for the variation of the hfcs in non-dipolar solvents like benzene and octadecane. The major difference between these two non-dipolar solvents is that benzene has a large molecular electric quadrupole moment while octadecane does not. We will therefore investigate the effect of solvent quadrupole moments on the hfcs of the cyclohexadienyl radical and extend the dipole−dipole reaction field model to include dipole−quadrupole interactions. The corresponding equations will be coupled with the predictions of ab initio calculations, and the results will be compared with the experiment.

It has been suggested that the temperature coefficient of the ^{14}N hfc of DTBN depends only on the variation of the solvent density with temperature.[23] One of the intentions of this study is to distinguish the factors that influence the A_p^{met} temperature behavior of C_6H_7, by comparing the temperature dependence of the A_p^{met} in the gas phase and the temperature dependence of the solvent density with the temperature dependence of the A_p^{met} in the solvent.

Experimental Details

Materials. All solvents except water were purchased from Aldrich and used without further purification. The triply distilled water used was prepared in our laboratory. All components were bubbled with N_2 and mixed in a glovebox under oxygen free conditions. The samples were prepared by mixing alcohols and water (in different volume ratios as given in Table 1) with the benzene, the concentration of which was 20 mM in all mixtures. This concentration was used so that the C_6H_6Mu radical did not interact with benzene molecules and the benzene concentration was below the solubility limit for all of the solvents (23 mM in water at $T = 298$ K, where it is the lowest).

ALC-μSR Experiments. Measurements were performed using the ALC spectrometer at the πE3 port of the Swiss Muon Source at the Paul Scherrer Institute in Villigen, Switzerland. Spectra were recorded over the field range appropriate for Δ_0 ALC resonances of the C_6H_7 methylene protons (typically 19 000−21 000 G, with 20 G steps) at 298, 323, and 348 K. For octadecane, the measurements were performed at 308 and 348 K because of its melting point ($T_m = 303$ K).

Data Processing and Analysis. The raw experimental data were corrected for the field dependent background by subtracting the spectrum of pure water (which contains no resonances) in the same field range. Afterward, the corrected data were fit with a single Lorentzian using the MINUIT function minimization library.[24]

The Δ_0 resonance field only provides the difference between A_μ and A_p. A_μ can be measured by transverse field muon spin rotation, but this is limited to solutions with a benzene concentration of greater than 0.1 M, which is significantly larger than the solubility of benzene in some solvents used in this study. Both the A_μ^{met} and the A_p^{met} were measured in neat benzene and in the gas phase. Yu et al. determined the ratio $S = (A_\mu/A_p)^{met} = 4.060 \pm 0.001$ in neat benzene,[20] while Fleming et al. found $S = 4.063$ at 313 K and 4.058 at 353 K in the gas phase.[21] S is primarily due to the γ_μ/γ_p ratio, which has a value of 3.183, with the remainder arising from the mass dependence of the internal dynamics. Since the vibrational modes of the two isotopologues are analogous, we assume that S is independent of solvent and temperature and use its value measured by Yu et al. to calculate the A_p^{met} values from the Δ_0 resonance field on the basis of

$$A_p^{met} = \frac{2B_r}{(S-1)/(\gamma_\mu - \gamma_p) - (S+1)/\gamma_e} \tag{4}$$

After substituting the values of S and the other constants, eq 4 can be simplified for the case of A_p^{met} to give

$$A_p^{met} = \frac{B_r}{163.76}\frac{\text{MHz}}{\text{G}} \tag{5}$$

This equation is only valid for the A_p^{met} of C_6H_6Mu as S depends on the structure and the vibrational frequencies of the radical.

The $[\mu_S] = \mu_S\rho_S/M_S$ values for mixtures depend on the volume fractions of the constituents in the following manner:

$$[\mu_S] = \frac{[\mu_S^{(1)}]V_1 + [\mu_S^{(2)}]V_2}{V_1 + V_2} \tag{6}$$

where V_1 and V_2 are the volumes of solvents in the mixtures and $[\mu_S^{(1)}]$ and $[\mu_S^{(2)}]$ are the dipole moment concentrations multiplied with the corresponding dipole values in the pure solvents. The $[\mu_S]$ values of the solvents and the mixtures studied here are given in Table 1. The overall dipole moment of aliphatic alcohols is very dependent on their conformation, and this may vary in various mixtures and liquids. In order to overcome this uncertainty, we will use the OH group dipole moment in the analysis, since the dipole moment of these alcohols is mainly located on the OH group. Its gas-phase value is $\mu_{OH} = 1.78$ D,[25] and this is the value that is used here. In order to be consistent, we decided to use the gas-phase value for water as well ($\mu_{water} = 1.855$ D).[26]

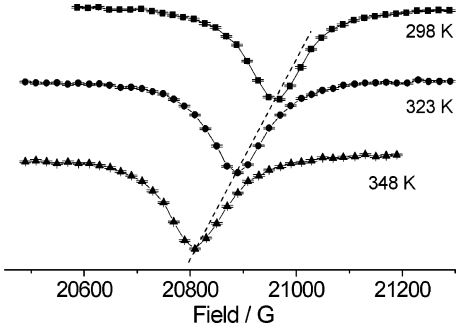

Figure 2. Temperature dependence of the cyclohexadienyl radical methylene proton Δ_0 ALC resonance in water.

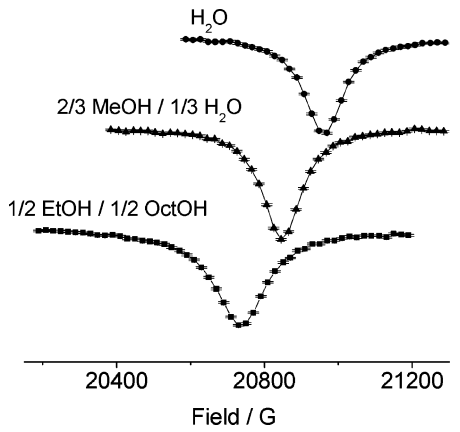

Figure 3. Selected ALC-μSR spectra of methylene proton Δ_0 ALC resonances at 298 K. Abbreviations: MeOH (methanol), EtOH (ethanol), and OctOH (octanol).

Ab Initio Calculations. Ab initio calculations were performed using the Gaussian 98 software package.[27] The unrestricted B3LYP method was used with the 6-311++G** basis set, as this combination has been demonstrated to predict hfcs that are in close agreement with experimental values.[28] Calculations were also performed with other basis sets to determine whether this influences the results, but no qualitative changes were observed so only the results with the 6-311++G** basis set are reported. In order to mimic the polarity range of different environments, the magnitude of the electric field introduced in the ab initio calculations was varied until the experimentally measured difference in A_p^{met} between octadecane and water was reproduced. The Mu atom was treated as a H atom.

Results

ALC-μSR. Δ_0 ALC-μSR resonance peak positions of the C_6H_7 methylene protons are listed in Table 1, and corresponding A_p^{met} values were extracted using eq 5. Their accuracy depends mainly on the validity of the approximation that $S = (A_\mu/A_p)^{met}$ remains the same in all solvents and mixtures. The methylene proton Δ_0 ALC-μSR resonance in water is shown for three temperatures in Figure 2. The resonance field decreases linearly with increasing temperature. The same behavior was observed in all of the other solvents and mixtures studied here, but the slopes are somewhat different, as seen in Table 1. The resonance fields were linearly extrapolated to 308 and 348 K and afterward used in the calculation of the hfcs. At constant temperature, the ALC Δ_0 resonance shifts toward lower magnetic fields with decreasing solvent polarity. Selected ALC-μSR spectra in different solvents are displayed in Figure 3, and the shift of the resonance field is linearly dependent on the $[\mu_S]$ value as presented in Table 1.

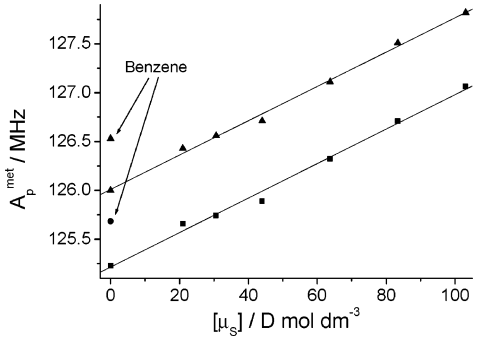

Figure 4. Cyclohexadienyl radical methylene proton hfcs as a function of the $[\mu_S]$ value at 308 K (▲) and 348 K (■). The experimental points are for the entries in Table 1.

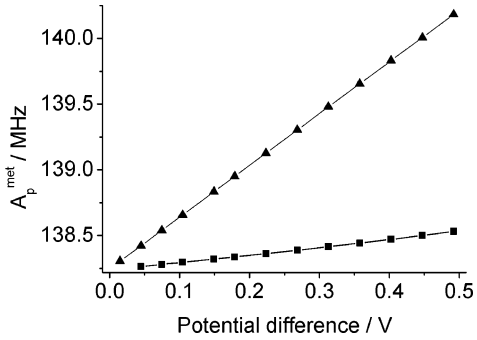

Figure 5. Dependence of the methylene proton hfc on the potential difference $\Delta U_{C^{met}-C^p}$ between the methylene and the para carbon atoms according to eq 13: (▲) in an electric field, $C' = 3.94$ MHz V^{-1} (structure allowed to optimize), (■) electric field off (with structure optimized in field), $C' = 0.59$ MHz V^{-1}.

In the water, neat alcohols, and the mixtures, A_p^{met} depends linearly on $[\mu_S]$, as shown in Figure 4. It is given by

$$A_p^{met}(T = 308\ \text{K}) = 126.01(3)\ \text{MHz} + 0.0176(5)\ \frac{\text{MHz·dm}^3}{\text{D·mol}} \times [\mu_S] \quad (7)$$

$$A_p^{met}(T = 348\ \text{K}) = 125.22(4)\ \text{MHz} + 0.0176(7)\ \frac{\text{MHz·dm}^3}{\text{D·mol}} \times [\mu_S] \quad (8)$$

where the units of $[\mu_S]$ are Debye mol dm^{-3}.

The intercepts with the ordinate and the slopes of eqs 7 and 8 correspond to the factors A and B of the RK theory (eq 2). It should be noted that B in this case is very sensitive to the value of the dipole moment.

A_p^{met} of the C_6H_6Mu radical in benzene does not match the trend observed for the other solvents and mixtures, since A_p^{met} is almost the same as that for ethanol, even though benzene has the same $[\mu_S]$ value as octadecane.

Ab Initio Calculations. A_p^{met} depends linearly on the potential difference between the methylene and the para carbon atoms with a slope, C', of 3.94 MHz V^{-1} (Figure 5). Absolute values of the hfcs obtained with the 6-311++G** basis set are closer to the experimentally observed values than those obtained using EPR II; however, in both cases, A_p^{met} depends linearly on the potential difference, and the slopes are approximately the same. The discussion below is based on calculations using 6-311++G**.

The structure of the C_6H_7 radical depends on the strength of the external electric field. This structure was optimized in various applied electric fields. Then, the field was set to zero,

and A_p^{met} was calculated for these field-optimized structures. In this case, the slope of the potential difference versus the external field was 6.6 times smaller than when optimization and hfc calculations were performed in the same electric field. This demonstrates that the effect of the electric field on the hfcs is much larger than the effect of the structural changes induced by the applied field.

The charge distribution, structure, and dipole moment of the C_6H_7 radical are perturbed by an applied electric field. The ab initio calculations with an applied electric field show that the dipole moments and A_p^{met} of C_6H_7 depend linearly on the electric field. The dependence of A_p^{met} on the C_6H_7 dipole moment, $\mu_{C_6H_7}$ (in Debye), is given by

$$A_p^{met} = 136.8\ \text{MHz} + 2.69405\ \frac{\text{MHz}}{\text{D}}\mu_{C_6H_7} \qquad (9)$$

In the range of electric fields introduced in these calculations, the C_6H_7 dipole moment changes from the 0.54 D (applied electric field $E = 0$ V m^{-1}) to 1.26 D (applied electric field $E = 1.7 \times 10^9$ V m^{-1} which is the necessary field to reproduce the full experimental A_p^{met} solvent shift). In the following, we will quote the potential difference between the methylene and the para carbon atoms which is related to the electrical field via $\Delta U_{C^{met}-C^p} = Ed_{C^{met}-C^p}$, where $d_{C^{met}-C^p} \approx 2.9 \times 10^{-10}$ m is the distance between the two carbon atoms.

The reliability of the ab initio calculations was checked by calculating the isotropic polarizability volume, α, of benzene from the dependence of the induced dipole moment in the electric field and averaging the results obtained with the field perpendicular and parallel to the six-membered ring. The experimentally measured isotropic polarizability volume of benzene is 1.03×10^{-29} m^3, while the value determined from the ab initio calculations is 1.17×10^{-29} m^3. The similarity of these values for the polarizability volumes allows us to conclude that the results obtained from ab initio calculations can be considered reliable. The polarizability volume of the C_6H_7 radical along the dipole moment is 1.27×10^{-29} m^3, which is close to the experimentally measured isotropic polarizability of benzene.

Discussion

Comparing the experimental data for A_p^{met} to the results of the ab initio calculations (Figures 4 and 5) reveals that the calculated values are too high by approximately 9%. There are several reasons for this: (i) The hfcs represent the difference between the densities of electron spin α and β at the nucleus, a difference between two large numbers which has always been difficult to evaluate, in particular, as the basis sets are better representations of the tails of the atomic wave functions than of the cusps at the nuclei. (ii) Because of its delocalized nature and the importance of spin polarization, quantum chemical calculations of the hfcs of C_6H_7 radical proved to be particularly difficult, and the predicted values for the methylene protons fluctuated by more than a factor 3 between the different methods.[29] (iii) Calculations relate to the rigid equilibrium geometry and a temperature of 0 K. While vibrational averaging and thermal population of vibrationally excited states is, in principle, possible, it is computationally demanding for the 33 internal degrees of freedom of C_6H_7, and it leads to contributions of both positive and negative sign. In the present case, the negative temperature dependence of the experimental A_p^{met} increases the discrepancy. Since the aim of the present study is an interpretation of changes on solvation rather than of absolute values of A_p^{met}, the mismatch of absolute values does not present a real problem.

In the continuum model, the hfcs only depend on the dielectric constant of the solvent,[8] so benzene and octadecane, which have similar dielectric constants, would be expected to have identical hfcs. This is not the case, as A_p^{met} is 0.45 MHz larger in benzene than in octadecane but similar to the value in the polar ethanol, as seen in Figure 4. Abe et al.[30] proposed that the reaction field of the induced dipole moment on the solvent molecule influences the radicals' hfcs so that it increases with the increasing polarizability. This hypothesis seems reasonable and will be further considered here, but it is also proposed that there are further solvent properties that are not included in the RK model but can alter the hfcs of a radical.

Comparison between DTBN and C_6H_7. There are several differences between the DTBN and the C_6H_7 radical that have to be considered. The charges responsible for the C_6H_7 dipole moment are spread over the whole molecule, while in the DTBN they are mostly localized on the NO group. Solvent molecules may approach C_6H_7 more closely than DTBN which is protected by the bulky *tert*-butyl groups. Nevertheless, DTBN can form strong hydrogen bonds along the axis of the NO group.

Hydrogen Bonding. Hydrogen bonding with the π electron system is of great importance in both chemical and biological recognition.[31,32] In the course of hydrogen-bonding interaction between the benzene and the water molecules, water molecules approach benzene from both sides of the aromatic ring.[32] Fluctuations of the hydrogen bonds occur on a time scale of $\sim 10^{-12}$ s,[33] whereas the time scale of the μSR experiment is on the order of 10^{-6} s, given by the muon lifetime. This means that experiments with C_6H_7 (in this case represented by C_6H_6Mu) monitor a time average which sees hydrogen bonding with equal probability from both sides of the ring plane. The components of the water dipole moment vector perpendicular to the C_6H_7 plane, therefore, cancel each other out, whereas the component parallel to the C_6H_7 long axis does not, because of symmetry reasons. A recent theoretical study of $C_6H_7-H_2O_n$ ($n = 1, 2$) clusters in the gas phase and in a continuum has shown an increase of the mean A_p^{met} for certain geometries, which is in qualitative agreement with our experiments.[34] According to this study, this hydrogen bond is found to be relatively weak.

With respect to the RK theory,[10] hydrogen bonding affects the hfcs of C_6H_7 if it produces a net electric field along the C_6H_7 dipole moment axis. Therefore, the orientation of the second oxygen−hydrogen bond of H_2O, that is, the one that is not hydrogen bonded to the C_6H_7 ring, is relevant. Straka et al.[34] also reported small changes in bond lengths between the methylene carbon and the hydrogen atoms, which also affects A_p^{met}. Furthermore, the dynamics of the system plays a paramount role.

Hydrogen bonding of the C_6H_7 radical is of significant importance in situations where it does not occur symmetrically with respect to the C_6H_7 ring plane, for example, when the radical resides on a hydroxylated silica gel surface.[35,36] In this case, the electric field due to the surface OH groups is, to a first approximation, perpendicular to the C_6H_7 ring plane. Therefore, the methylene protons are no longer equivalent, and it is expected that methylene bond lengths and angles differ from those in the gas and in the liquid phase. Experimentally in a monolayer of benzene, an increase of A_μ^{met} of C_6H_6Mu amounting to 0.4% (0.5 MHz relative to neat benzene) is observed.[36] This corresponds to about 1/3 of the difference between neat benzene and bulk water.

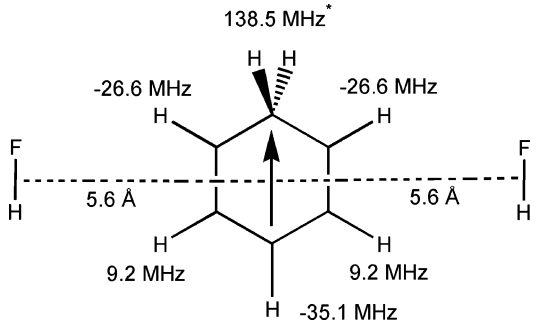

Figure 6. Results of ab initio calculations when the dipole moments are placed on either side and antiparallel with respect to the dipole moment of the cyclohexadienyl radical. The hfcs are written next to the corresponding atoms for the given configuration. Arrow represents the dipole moment direction of the cyclohexadienyl radical. Asterisk: gas phase (field = 0); $A_p^{met} = 138.2$ MHz.

Dipole−Dipole Reaction Field Model. The benzene molecule is centrosymmetric, whereas C_6H_7 has a dipole moment between 0.54 D (in vacuum, no electric field) and 1.26 D (at 1.7×10^9 V m^{-1}, the highest electric field applied in this study). C_6H_7 is, thus, moderately polar and can polarize its environment via the dipole−ion, dipole−dipole, dipole−induced dipole, and dipole−quadrupole interactions. Water has a pK_a value of 14, which means that the concentration of dissociated molecules is 10^{-7} M. The fraction of dissociated molecules in alcohols is even smaller. Therefore, dipole−ion interactions will not be taken into account.

C_6H_6 and C_6H_7 are of similar shape. The mean distance of the first solvent shell of neat benzene, 5.6×10^{-10} m, is chosen as an approximate distance between the dipole moments of the C_6H_7 radical and of the solvents.[37] The dipole−dipole electrostatic interaction ($E_{d-d} \sim 1/r^3$) of the two dipole moments ($\mu_{C_6H_7} = 1.26$ D and $\mu_{H_2O} = 1.855$ D) varies between the $E_{d-d} = 0$ and $E_{d-d} = 1.6$ kJ mol^{-1}, depending on the relative orientation. This is significant compared to the thermal energy in the temperature range of the present study ($RT = 2.56$ kJ mol^{-1} at 308 K and 2.89 kJ mol^{-1} at 348 K).

The dipole−induced dipole interaction energy ($E_{d-id} \sim 1/r^6$) is several orders of magnitude smaller than E_{d-d} for the C_6H_7 radical in water ($E_{d-id} \approx 0.01$ kJ mol^{-1}) and is, therefore, negligible. In alcohols, this interaction may be larger since the alkyl part of the solvent molecules becomes bigger (polarizability increased), but it remains insignificant compared to the dipole−dipole interaction. The dipole−quadrupole interaction ($E_{d-q} \sim 1/r^4$) is of importance in solvents of significant quadrupole moments, as discussed further below. The dipole moment of the C_6H_7 radical will induce an alignment of neighboring solvent dipoles, and thermal energy works against this alignment. The liquid system represents a dynamical equilibrium on the time scale of the μSR experiment ($\approx 10^{-6}$ s). The interaction between C_6H_7 and water or the alcohols is comparable to thermal energy at room temperature, so the neighboring solvent molecules do exhibit preferred but incomplete orientations, which results in a net electric field along the direction of the dipole moment of C_6H_7.

We investigated the effect of the solvent molecules' dipole moments arranged in selected geometries as shown in Figures 6 and 7. Within the point dipole approximation, the effective contribution of this arrangement to the electrostatic potential (and corresponding potential difference) may be calculated using

$$U = \frac{1}{4\pi\epsilon_0}\frac{\mu_S}{r^2}\cos\theta \qquad (10)$$

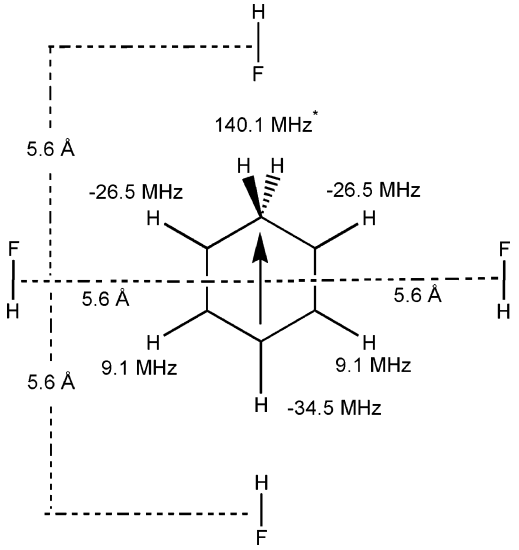

Figure 7. Results of ab initio calculations when the dipole moments are placed parallel and on either side antiparallel with respect to the cyclohexadienyl radical dipole moment axis. The hfcs are written next to the corresponding atoms for the given configuration. Arrow represents the dipole moment direction of the cyclohexadienyl radical. Asterisk: gas phase (field = 0); $A_p^{met} = 138.2$ MHz (structures of the molecules in the figure were previously optimized in the gas phase).

where μ_S is the molecular dipole moment of the solvent and θ is the angle between its direction and the axis that connects the solvent dipole moment and the C_6H_7 center.[38] In the arrangement of Figure 6, the angle θ is 90°, and the contribution to the electrostatic potential is zero.

More accurate calculations require including the molecular shape and a realistic charge distribution in the molecule, and this was done with ab initio calculations for the C_6H_7 radical with several neighboring polar molecules as shown in Figures 6 and 7. Hydrofluoric acid (HF) was used because it has a dipole moment of similar magnitude to that of water, and its simple structure and charge distribution gives a straightforward picture of the electric field direction. The structures of the molecules in Figure 6 were first optimized in vacuum. The arrangement shown in Figure 6 has a negligible effect on A_p^{met}. Another arrangement of the C_6H_7 radical and neighboring molecules where two dipole moments were placed antiparallel aside and two were placed parallel on the axis of the C_6H_7 dipole moment as shown in Figure 7 was also explored. The molecules on the dipole moment axis have a much larger effect on the hfc than the off-axis molecules. This was one of the results of the RK dipole−dipole reaction field model. It is due to the cosine in eq 10 that equals unity along the dipole moment axis but is zero for the off-axis solvent molecules.

Now, we test the RK model for the case of C_6H_7 in the liquids. The in-plane ring protons reside in the nodal plane of the π system at zero nominal spin density from the semioccupied molecular orbital (SOMO). They acquire their nonzero hfc via spin polarization of the remaining π and the σ system, and the value of the hfc is proportional to the spin population at the adjacent carbon atom. In contrast, the two methylene hydrogen atoms are one above and one below the ring plane. A negative linear combination of their 1s wave functions has π symmetry and conjugates into the carbon π system. C_6H_7 is, thus, properly regarded as a seven-electron rather than a five-electron π system.[39] Much of the methylene proton hfc arises from direct spin density in the SOMO.[29] Nevertheless, the ab initio calculations show that A_p^{met} is directly proportional to the spin population ρ_C^{met} at the methylene carbon:

$$A_p^{met} = A_p^{0\prime} + c\rho_{C^{met}} \quad (11)$$

where $A_p^{0\prime} = 197.77$ MHz and $c = 569$ MHz are constants typical for the radical and $\rho_{C^{met}}$ is of the order of -0.103. When the RK model is applied, both A_p^{met} and $\rho_{C^{met}}$ should depend linearly on the electric potential difference between the methylene and the para carbon atom, $\Delta U_{C^{met}-C^p}$:

$$\rho_{C^{met}} = a + b\Delta U_{C^{met}-C^p} \quad (12)$$

, and this is exactly what we derive also from the ab initio calculations. Constants a and b are typical for the system. Introducing eq 12 in eq 11, we obtain

$$A_p^{met} = A_p^{0} + C'\Delta U_{C^{met}-C^p} \quad (13)$$

where $A_p^0 = A_p^{0\prime} + ac$ and $C' = cb$. This linear dependence of A_p^{met} on ΔU was confirmed from the ab initio calculations shown in Figure 5, and the values of A_p^0 and C' were determined to be 138.25 and 3.94 MHz V^{-1}, respectively.

Using the same mathematical treatment as RK results in an equation of the same form as eq 2 but with somewhat different constants. Thus, it may be concluded that the RK dipole−dipole reaction field model is appropriate to describe the solute−solvent interactions for the C_6H_7 radical since A_p^{met} depends linearly on the concentration of the dipole moments multiplied with the magnitude of the dipole moment (Figure 4 and eqs 7 and 8) and A_p^{met} is linearly dependent on the potential difference along the radicals' dipole moment (Figure 5).

Dipole−Quadrupole Reaction Field Model. A_p^{met} of C_6H_7 in benzene is 0.45 MHz larger than the corresponding value in octadecane and 0.7 MHz larger than the value in the gas phase (124.9 MHz at $T = 308$ K).[21] This indicates that the potential difference in benzene is 0.18 V larger than in the gas phase and 0.13 V larger than in octadecane (assuming octadecane as an environment with zero reaction field, which disregards the effect of the weaker van der Waals forces).

In Figure 8, two preferential orientations of C_6H_7 and C_6H_6 are shown. In the upper one, the negative sector of the benzene quadrupole moment is oriented toward the positive end of the C_6H_7 dipole moment. In the second case, the positive sector of the quadrupole moment is oriented toward the negative end of the dipole moment. These two arrangements correspond to energy minima; however, the treatment below takes into account all relative orientations. Our analysis is based on the formalism introduced by Buckingham.[38] The average reaction field and the corresponding electric potential difference due to the solvent molecule electric quadrupole moment (in this case benzene) on the solutes' dipole moment (in this case the C_6H_7 radical) are calculated from the Boltzmann distribution.

The energy of the dipole−quadrupole interaction (E_{d-q}) can be described by[38]

$$E_{d-q} = \frac{1}{4\pi\epsilon_0}\frac{3}{2r^4}Q_S\mu_{Solute}(\cos\alpha(3\cos^2\beta - 1) + 2\sin\alpha\sin\beta\cos\beta\cos\gamma) \quad (14)$$

where Q_S and μ_{Solute} are the molecular electric quadrupole and the electric dipole moments of solvent and solute molecules, respectively, r is the distance between their centers, and ϵ_0 is the vacuum dielectric constant. α, β, and γ are the angles between the quadrupole moment and the dipole moment symmetry axes as defined in Figure 9.

The relative orientation of the solvent electric quadrupole and of the solutes' electric dipole moment axes is given by the probability dW:

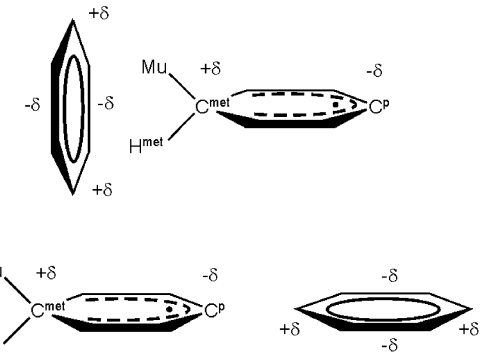

Figure 8. Arrangements of the benzene and the cyclohexadienyl radical (partial charge distribution simplified as in the figure).

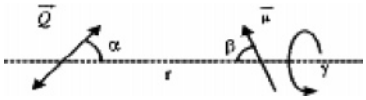

Figure 9. Orientation of the dipole moment vector and quadrupole moment tensor and corresponding angles.

$$dW_{Quad-Dip} = \frac{\exp\left(-\frac{E_{d-q}(\alpha,\beta,\gamma)}{k_BT}\right)}{\int_0^{2\pi}\int_0^{2\pi}\int_0^{2\pi}\exp\left(-\frac{E_{d-q}(\alpha,\beta,\gamma)}{k_BT}\right)d\alpha\,d\beta\,d\gamma}\,d\alpha\,d\beta\,d\gamma \quad (15)$$

where k_B is the Boltzmann constant. The electric (reaction) field, R_{Quad}^{Field}, produced by the quadrupole moment at a fixed average distance, r, is[38]

$$R_{Quad}^{Field} = \frac{|Q_S|}{4\pi\epsilon_0 r^4}\frac{(3\cos^2\alpha - 1)}{2} \quad (16)$$

The Boltzmann averaged reaction field that is due to the quadrupole moment of a single solvent molecule, $\overline{R_{Quad-Dip}^{Field}}$, on the solute dipole can therefore be written as

$$\overline{R_{Quad-Dip}^{Field}} = \frac{|Q_S|}{4\pi\epsilon_0 r^4}\int_0^{2\pi}\int_0^{2\pi}\int_0^{2\pi}\frac{(3\cos^2\alpha - 1)}{2}\times \frac{\exp\left(-\frac{E_{d-q}(\alpha,\beta,\gamma)}{k_BT}\right)}{\int_0^{2\pi}\int_0^{2\pi}\int_0^{2\pi}\exp\left(-\frac{E_{d-q}(\alpha,\beta,\gamma)}{k_BT}\right)d\alpha\,d\beta\,d\gamma}\,d\alpha\,d\beta\,d\gamma \quad (17)$$

For the contribution of two solvent molecules located on the solute molecule dipole moment axis, eq 17 can be expressed for numerical treatment as

$$\overline{R_{Quad-Dip}^{Field}} = \frac{|Q_S|}{4\pi\epsilon_0 r^4}\sum_0^{2\pi}\sum_0^{2\pi}\sum_0^{2\pi}(3\cos^2\alpha - 1)\times \frac{\exp\left(-\frac{E_{d-q}(\alpha,\beta,\gamma)}{k_BT}\right)}{\sum_0^{2\pi}\sum_0^{2\pi}\sum_0^{2\pi}\exp\left(-\frac{E_{d-q}(\alpha,\beta,\gamma)}{k_BT}\right)d\alpha\,d\beta\,d\gamma}\,d\alpha\,d\beta\,d\gamma \quad (18)$$

The potential difference is approximated with the electric field at the center of the C_6H_7 radical and the distance between the methylene and the para carbons of the C_6H_7 radical (as previously done for the case of DTBN by RK):[10]

$$\Delta U = \overline{R^{\text{Field}}_{\text{Quad-Dip}}} d_{C^{\text{met}}-C^{\text{p}}} \quad (19)$$

$\overline{R^{\text{Field}}_{\text{Quad-Dip}}}$ is calculated using the mean distance from the radial distribution function (RDF) of liquid benzene for an estimate of the distance r between the C_6H_7 solute and the benzene solvent molecule. Several molecular dynamics studies have been reported, and there is good agreement among these studies and the observed values.[40] The first peak of the RDF, from which the distance is deduced, does not change significantly with temperature. Though benzene is an anisotropic molecule, a significant dependence of the RDF on the relative orientation is not observed. A shortcoming of this approach is that it neglects the significant dipole moment of C_6H_7. Therefore, there should be a larger angular dependence of the RDF in this system, and the molecules would be closer to each other because of the additional dipole−quadrupole interaction between the C_6H_7 radical and benzene.

Using the value of $r \approx 5.6 \times 10^{-10}$ m as recommended by Chelli et al.,[37] $Q_{\text{benzene}} = -2.9 \times 10^{-39}$ C m^{+2},[41] $d_{C^{\text{met}}-C^{\text{p}}} \approx 2.9 \times 10^{-10}$ m, and $\mu_{C_6H_7} \approx 1$ D, we obtain, with the help of appropriate numerical routines,[42] a potential difference $\Delta U \approx 0.04$ V. This is 23% of what is required to give the necessary increase of the hfc of 0.70 MHz, but the calculation depends critically on the solute−solvent distance, as it scales inversely with its fourth power (eq 17). Therefore, calculating the potential difference with a fixed value of r may not lead to a fully correct absolute value, but it may be used for estimating the relative differences among the quadrupolar liquids.

We furthermore note that r generally scales with the cube root of the inverse concentration. Inserted into eq 18, this means that the reaction field in quadrupolar solvents is proportional to the concentration of quadrupolar solvent molecules to the 4/3 power.

A further origin of the discrepancy between calculation and experimental results is that the electric point dipole and the electric point quadrupole moment approximations are not entirely valid on such a small distance between molecules.

The agreement between the calculated (with the help of eq 19) and the necessary potential difference (obtained from the results of ab initio calculations, Figure 5) may still be considered as remarkably good, having in mind the uncertainty in the parameters used and the assumptions made in the calculations.

We further suggest that other molecular properties of nondipolar liquids should be used in the evaluation of the solvent−solute interactions such as higher multipoles, unusually large polarizability, and preferred solute−solvent arrangements as well.

Influence of the Structure. The presence of the electric field from the solvent molecule in the vicinity of C_6H_7 is expected to induce small changes in the structure of this relatively rigid radical, which in return influences the hfcs. There are three main variables in the system that can influence the A_p^{met}: (i) the distance between the methylene and the para carbon, (ii) the methylene C−H bond length, and (iii) the bond angle between the methylene C−H bonds. It is very difficult to distinguish between these contributions, since the electronic structure of this radical is a function of numerous bond angles and bond lengths, some of which increase and some decrease the hfcs.[34] It can be seen in Figure 5 that the contribution due to electric field induced changes of the radical structure amounts to ≈15% of the overall hfc change. The change of the $C^{\text{met}}-C^{\text{p}}$ distance with electric field is very small, as seen in Figure 10. The change of the $C^{\text{met}}-H^{\text{met}}$ bond length and of the angle between methylene C−H bonds is also small (not shown here; it was also noticed by Straka et al. for the $C_6H_7-H_2O$ complexes[34]), but as can be seen from Figure 5, even small structural changes can have a considerable effect on hfcs.

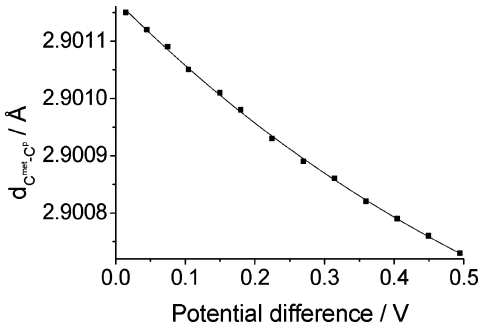

Figure 10. Ab initio results of the dependence of the methylene and para carbon atom distance (C^{met} and C^{p} in Figure 1) on the potential difference between the two atoms.

Comparison with Other Cyclohexadienyl-Type Radicals. In the studies of Mu adducts to phenylethanol (PEA-Mu) and phenylpentanol (PPA-Mu), the A_p^{met} of all isomers (para, ortho, and meta with respect to the Mu addition site) were observed to depend approximately linearly on the concentration of the OH groups in solvents of different polarities.[15,12] The largest deviations from linearity were observed for the case of the para PEA-Mu isomer. It was shown that the substituent group plays an important role and contributes to the deviations from linearity. Solute−solvent interactions originating in the microscopic solvent properties, preferential solvation, and different hydrogen-bonding effects may lead to this deviation.[15] For the range of alcohols used in the present study, the behavior of A_p^{met} of the C_6H_7 radical and that of the PEA-Mu and PPA-Mu radicals is similar.[12,15] In these solvents, they all exhibit a linear dependence on the dielectric constant as well.[12] It was shown previously that the dielectric constants of the alcohols and mixtures used in the present study and in the studies of PEA-Mu and PPA-Mu radicals are directly proportional to the concentration of the OH groups.[43]

A very similar result would be obtained if the $[\mu_S] = \mu\rho/M_S$ value was used because of the fact that the dipole moments of the solvent molecules in these studies are of similar magnitude. However, the A_p^{met} of the PEA-Mu radicals in ethylacetate[12] do not follow the proportionality to the dielectric constant ($\epsilon_{\text{ethylacetate}} = 6.0$) or to the concentration of OH groups (which is zero for ethylacetate).[12] Using $[\mu_S]$ as recommended in the present study ($[\mu_S]_{\text{ethylacetate}} = 18.2$ D mol dm^{-3}) brings this point close to the linear trend.

Temperature Effects. The observed hfc of a radical represents a vibrational average over all of the internal degrees of freedom, and increased temperature leads to more extensive vibrational motion. The A_p^{met} of C_6H_7 increases linearly with temperature primarily because of the increased amplitude of the methylene scissor motion.[20] The contribution to the temperature dependence of the A_p^{met} due to vibrational effects is denoted as $(\Delta A_p^{\text{met}}/\Delta T)_{\text{VIB}}$.

Furthermore, increased temperature leads to greater disorder in a liquid, and this will result in a decrease in the external electric field and a lower hfc. This contribution is denoted as $(\Delta A_p^{\text{met}}/\Delta T)_{\text{HT}}$.

The hfc is also sensitive to the distance between the radical and the neighboring solvent molecules. The density of a liquid generally decreases with increasing temperature, and this leads to a larger radical−solvent distance, a decreased [μ_S] value, and a lower hfc. The densities of the liquids studied in this experiment decrease to a first approximation linearly with temperature. The contribution due to the decreased density is denoted as $(\Delta A_p^{met}/\Delta T)_{DEN}$.

The change of the A_p^{met} due to vibrational averaging, $(\Delta A_p^{met}/\Delta T)_{VIB}$, will be approximately the same in all solvents, assuming that rigidness of the cavity does not influence the structure. $(\Delta A_p^{met}/\Delta T)_{HT}$ and $(\Delta A_p^{met}/\Delta T)_{DEN}$ are unique for each solute−solvent mixture. It is reasonable to assume that all of these effects contribute independently to the temperature dependence of the A_p^{met}, as shown in the following equation:

$$\frac{\Delta A_p^{met}}{\Delta T} = \left(\frac{\Delta A_p^{met}}{\Delta T}\right)_{VIB} + \left(\frac{\Delta A_p^{met}}{\Delta T}\right)_{HT} + \left(\frac{\Delta A_p^{met}}{\Delta T}\right)_{DEN} \quad (20)$$

We will discuss the temperature dependence of A_p^{met} in water as a typical example, where $(\Delta A_p^{met}/\Delta T)_{water} = -0.0183$ MHz K^{-1} (Table 1).

The absence of any intermolecular interactions in the gas phase means that the hfc temperature dependence is entirely due to vibrational excitation, $(\Delta A_p^{met}/\Delta T)_{VIB}$. Assuming that the intramolecular vibrations remain the same in the gas and in the liquid, it is possible to estimate the influence of these effects by comparing the results of studies of A_p^{met} in the gas phase with our studies. Fleming et al. determined that the temperature dependence of the A_p^{met} in the gas phase is -0.0125 MHz K^{-1} or ≈68% of the effect in water when compared with our experiments.[21]

By differentiating eq 2, it is possible to determine the contribution of the density change:

$$\left(\frac{\Delta A_p^{met}}{\Delta T}\right)_{DEN} = B\frac{\mu_S}{M_S}\frac{\Delta \rho_S}{\Delta T} \quad (21)$$

We now use eq 21 for the experimentally obtained dependence of A_p^{met} on [μ_S] at $T = 308$ K (eq 7). This coefficient remains almost exactly the same at $T = 348$ K (eq 8).

In the temperature range studied here, the water density is approximately proportional to the temperature. After introducing this coefficient and other constants ($\Delta\rho_S/\Delta T(H_2O) = -0.442\ 61$ g K^{-1} dm^{-3}, $\mu_S = 1.85$ D, and $M_S(H_2O) = 18$ g mol^{-1}) into eq 21, it is found that $(\Delta A_p^{met}/\Delta T)_{DEN} = -0.0008$ MHz K^{-1}, which accounts for ≈4% of the total effect (questioning significantly the conclusion reached by Griller[23]). The remaining temperature effect then has to be attributed to the increased solvent disorder, $(\Delta A_p^{met}/\Delta T)_{HT}$, and it amounts to approximately 28% of the total effect. The factors influencing the hfcs temperature dependence can be resolved in a similar way for every solvent and mixture.

Conclusions

The methylene proton and muon hfcs of the cyclohexadienyl radical were measured in neat solvents and mixtures of various polarities between octadecane and water and were found to be directly proportional to the concentration of the dipole moments and the magnitude of the dipole moment.

The hfcs of the cyclohexadienyl radical methylene protons are directly proportional to the potential difference between the methylene and the para carbon atoms (defined in Figure 1), which is caused by the electric field that results from partial ordering of the dipole moments of the neighboring solvent molecules. The solvent molecules on the long axis of the cyclohexadienyl radical dominate the interaction in this solute−solvent system. Approximately 15% of the change of the methylene proton hfc is due to changes in the radical structure in the applied electric field.

The quadrupole moment of a solvent can have a large effect on the hfcs of the C_6H_7 radical and can be the dominant interaction in non-dipolar solvents such as benzene. A dipole−quadrupole reaction field model has been developed to account for the variation of the hfcs of dipolar solutes in non-dipolar quadrupolar solvents. This model suggests that the reaction field scales with the product of the magnitude of the quadrupole moment and its concentration, $[Q_S]^{4/3}$, while in the case of the dipole moment, scaling with [μ_S] is linear.

The temperature behavior of the methylene proton hfc is mainly influenced by the thermal population of vibrational modes (≈68% of the effect) and increased disorder of the neighboring solvent molecules because of the increased temperature (≈28% of the effect). The influence of the temperature dependence of the solvent density is almost negligible (≈4% of the effect).

The approach of the present study has several advantages in comparison with the typically used continuum models.[8,22] It takes into account the fact that the radical hfcs in liquids of similar dielectric constant may be very different, and it is in better agreement with the experimental results. The advantage, in comparison with the study where the polarized continuum model with explicitly introduced water molecules is used,[34] is that it takes into account the behavior not just in the hydrogen-bonding liquids.

This approach is general since it describes the role of the electric field originating from the solvent molecules in the radical−solvent interaction. The influence of electric fields on radicals may be of importance but not only in liquid-like environments. Our study emphasizes the use of individual physical properties of the solvent molecules, such as the electric dipole and quadrupole moments (or exceptionally large polarizability), in describing solute−solvent interactions. Furthermore, we showed that the interaction of one class of solvents may be approximated by that of the dominating solvent property.

It is sometimes necessary in chemical synthesis to have large reaction fields, which is usually achieved by using dipolar liquids. This study clearly shows how it is possible to achieve such fields in non-dipolar solvents by using molecules with large electric multipole moments. This can be significant in cases where the solubility of reactants in dipolar liquids is the limiting factor.[44]

We suggest that the dipole−dipole reaction field model and its extension to include the dipole−quadrupole interactions is valid for other molecules and radicals as well. The potential radicals for which these models should be valid must be rigid because conformational changes can induce much larger differences of hfcs.[45] This radical should possess a dipole moment of considerable magnitude as well, to be able to cause some ordering in its vicinity.

Acknowledgment. Support by A. Stoykov from the Laboratory for Muon Spin Spectroscopy at the Paul Scherrer Institute is gratefully acknowledged. We thank the Deutsche Forschungsgemeinschaft for financial support for D.V. within the Research Training Group Nr. 448 at the University of Stuttgart. This research project was also supported by the European Commission under the 6th Framework Programme through the Key

Action: Strengthening the European Research Area, Research Infrastructures. Contract No. RII3-CT-2003-505925′. Also, I.M. thanks the Natural Sciences and Engineering Research Council of Canada for a postdoctoral fellowship.

References and Notes

(1) Lazar, M.; Klimo, V.; Rychly, J.; Pelikan, P. *Free Radicals in Chemical Biology*; CRC Press: Boca Raton, FL, 1989.

(2) Litwinienko, G.; Ingold, K. U. *J. Org. Chem.* **2004**, *60*, 5889.

(3) Yorimitsu, H.; Nakamura, T.; Shinokubo, H.; Oshima, K.; Omoto, K.; Fujimoto, H. *J. Am. Chem. Soc.* **2000**, *122*, 11041.

(4) Li, C. J.; Chen, L. *Chem. Soc. Rev.* **2006**, *35*, 68.

(5) Tomasi, J.; Mennucci, B.; Cammi, R. *Chem. Rev*. **2005**, *105*, 2999; see also references therein.

(6) Onsager, L. *J. Am. Chem. Soc.* **1936**, *58*, 1486.

(7) Kirkwood, J. G. *J. Chem. Phys.* **1934**, *2*, 767.

(8) Al-Bala'a, I.; Bates, R. D., Jr. *J. Magn. Reson.* **1987**, *73*, 78.

(9) Jeon, J.; Kim, H. J. *J. Chem. Phys.* **2003**, *119*, 8606.

(10) Reddoch, A. H.; Konishi, S. *J. Chem. Phys.* **1979**, *70*, 2121.

(11) Marsh, D. *Eur. Biophys. J.* **2002**, *31*, 559.

(12) Scheuermann, R.; Tucker, I. M.; Dilger, H.; Staples, E. J.; Ford, G.; Fraser, S. B.; Beck, B.; Roduner, E. *Langmuir* **2004**, *20*, 2652.

(13) Martyniak, A.; Scheuermann, R.; Dilger, H.; Tucker, I. M.; Burkert, T.; Hashmi, A. S. K.; Vujošević, D.; Roduner, E. *Physica B* **2006**, *374*−*375*, 328.

(14) Dilger, H.; Martyniak, A.; Scheuermann, R.; Vujošević, D.; Tucker, I. M.; McKenzie, I.; Roduner, E. *Physica B* **2006**, *374*−*375*, 317.

(15) Vujošević, D.; Scheuermann, R.; Dilger, H.; Tucker, I. M.; Martyniak, A.; McKenzie, I.; Roduner, E. *Physica B* **2006**, *374*−*375*, 295.

(16) Tolkachev, V. A.; Molin, Y. N.; Tchkeidze, I. I.; Buben, N. Y.; Voevodsky, V. V. *Dokl. Akad. Nauk SSSR* **1961**, *141*, 911.

(17) Fessenden, R. W.; Schuler, R. H. *J. Chem. Phys.* **1963**, *38*, 773.

(18) Percival, P. W.; Kiefl, R. F.; Kreitzman, S. R.; Garner, D. M.; Cox, S. F. J.; Luke, G. M.; Brewer, J. H.; Nishiyama, K.; Venkateswaran, K. *Chem. Phys. Lett.* **1987**, *133*, 465.

(19) Roduner, E.; Reid, I. D. *Isr. J. Chem.* **1989**, *29*, 3.

(20) Yu, D.; Percival, P. W.; Brodovitch, J.-C.; Leung, S. K.; Kiefl, R. F.; Venkateswaran, K.; Cox, S. F. J. *Chem. Phys.* **1990**, *142*, 229.

(21) Fleming, D. G.; Arseneau, D. J.; Pan, J. J.; Shelley, M. Y.; Senba, M.; Percival, P. W. *Appl. Magn. Reson.* **1997**, *13*, 181.

(22) Owenius, R.; Engström, M.; Lindgren, M.; Huber, M. *J. Phys. Chem. A* **2001**, *105*, 10967.

(23) Griller, D. *J. Am. Chem. Soc.* **1978**, *100*, 5240.

(24) *MINUIT-Function Minimization and Error Analysis*, version 96.03; CERN Program Library Entry D506; CERN: Geneva, Switzerland, 1996.

(25) Bader, R. F. W.; Keaveny, I.; Cade, P. E. *J. Chem. Phys*. **1967**, *47*, 3381.

(26) Lovas, F. J. *J. Phys. Chem. Ref. Data* **1978**, *7*, 1445.

(27) Frisch, M. J.; Trucks, G. W.; Schlegel, H. B.; Scuseria, G. E.; Robb, M. A.; Cheeseman, J. R.; Zakrzewski, V. G.; Montgomery, J. A., Jr.; Stratmann, R. E.; Burant, J. C.; Dapprich, S.; Millam, J. M.; Daniels, A. D.; Kudin, K. N.; Strain, M. C.; Farkas, O.; Tomasi, J.; Barone, V.; Cossi, M.; Cammi, R.; Mennucci, B.; Pomelli, C.; Adamo, C.; Clifford, S.; Ochterski, J.; Petersson, G. A.; Ayala, P. Y.; Cui, Q.; Morokuma, K.; Malick, D. K.; Rabuck, A. D.; Raghavachari, K.; Foresman, J. B.; Cioslowski, J.; Ortiz, J. V.; Stefanov, B. B.; Liu, G.; Liashenko, A.; Piskorz, P.; Komaromi, I.; Gomperts, R.; Martin, R. L.; Fox, D. J.; Keith, T.; Al-Laham, M. A.; Peng, C. Y.; Nanayakkara, A.; Gonzalez, C.; Challacombe, M.; Gill, P. M. W.; Johnson, B. G.; Chen, W.; Wong, M. W.; Andres, J. L.; Head-Gordon, M.; Replogle, E. S.; Pople, J. A. *Gaussian 98*, revision A.11; Gaussian, Inc.: Pittsburgh, PA, 1998.

(28) Improta, R.; Barone, V. *Chem. Rev.* **2004**, *104*, 1231.

(29) Chipman, D. *J. Phys. Chem.* **1992**, *96*, 3294.

(30) Abe, T.; Tero-Kubota, S.; Ikegami, Y. *J. Phys. Chem.* **1982**, *86*, 1358.

(31) Meyer, E. A.; Castellano, R. K.; Diederich, F. *Angew. Chem., Int. Ed*. **2003**, *42*, 1210; see also references therein.

(32) Raschke, T. M.; Levitt, M. *Proc. Natl. Acad. Sci. U.S.A.* **2005**, *102*, 6777.

(33) Keutsch, F. N.; Saykally, R. J. *Proc. Natl. Acad. Sci. U.S.A.* **2001**, *98*, 10533.

(34) Straka, M.; Kaupp, M.; Roduner, E. *Theor. Chem. Acc*. **2005**, *114*, 318.

(35) Schwager, M.; Roduner, E.; Reid, I. D.; Kreitzman, S. R.; Percival, P. W.; Brodowitch, J.-C.; Leung, S.-K.; Sun-Mack, S. *Z. Phys. Chem.* **1995**, *190*, 29.

(36) Schwager, M.; Dilger, H.; Roduner, E.; Reid, I. D.; Percival, P. W.; Baiker, A. *Chem. Phys.* **1994**, *189*, 697.

(37) Chelli, R.; Cardini, G.; Ricci, M.; Bartolini, P.; Righini, R.; Califano, S. *Phys. Chem. Chem. Phys.* **2001**, *3*, 2803.

(38) Buckingham, A. D. *Q. Rev. Chem. Soc.* **1959**, *13*, 183.

(39) Roduner, E. *The Positive Muon as a Probe in Free Radical Chemistry* − *Potential and Limitations of the μSR Techniques* (*Lecture Notes in Chemistry*); Springer: Berlin, 1988; Vol. 49.

(40) Cabaço, M. I.; M. I.; Danten, Y.; Besnard, M.; Guissani, Y.; Guillot, B. *J. Phys. Chem. B* **1997**, *101*, 6977; see also references therein.

(41) Battaglia, M. R.; Buckingham, A. D.; Williams, J. H. *Chem. Phys. Lett.* **1981**, *78*, 421.

(42) *Mathematica 5.2*; Wolfram Research, Inc.: Champaign, IL, 2006.

(43) Mukerjee, P.; Ramachandran, C.; Pyter, R. A. *J. Phys. Chem*. **1982**, *86*, 3189.

(44) Reichardt, C. *Solvents and Solvent Effects in Organic Chemistry*, 2nd ed.; Verlag Chemie: Weinheim, Germany, 1988.

(45) Krusic, P. J.; Meakin, P.; Jesson, J. P. *J. Phys. Chem.* **1971**, *75*, 3438.